JPEDAV (2007) 28:79–89
DOI: 10.1007/s11669-006-9008-3
1547-7037 ©ASM International

Configurational Entropies of Mixing in Solid Alloys

W. A. Oates

(Submitted October 25, 2006)

Entropy becomes an increasingly important contributor to the Gibbs energy at high temperatures with both non-configurational and configurational contributions to be considered. Some examples of where configurational entropies alone are important in determining the domain of phase stability of a solution phase are given. In phenomenological calculations, the modeling of configurational entropy should allow for short range order and be readily applicable to multi-component systems. The use of Fowler-Yang-Li transforms is important in this regard by providing the opportunity for changing the functional variables in cluster calculations of the Gibbs energy from cluster probabilities or correlation functions to the considerably fewer point probabilities, just as in the Bragg-Williams approximation.

Keywords alloys, chemical potentials, entropy, thermodynamics

1. Introduction

Metallurgy students of my generation were strongly influenced by the monographs of Prof. Hume-Rothery.[1-5] His name will always be particularly remembered for his work on first isolating the principal factors responsible for the stability of alloy phases. In the first editions of these monographs, there is no mention of any role for entropy, S, in determining phase stability, although Gibbs energies, G, are mentioned in the later, co-authored, editions.[6-8] The awareness of the important contribution of S has become much more widely recognized since then and, in this Lecture, I will concentrate on some aspects of its role in determining high temperature phase stability.

Although the contributions made by solid state physicists over the last two decades in the '*ab initio*' calculation of alloy phase stabilities has been outstanding, it seems clear that some degree of empiricism will continue to be important for some years to come in the evaluation and description of high temperature phase stabilities. The required accuracies in calculated Gibbs energies of just a few joules per mole of alloy at temperatures in the region of 1,000 K are still some way off the accuracy attainable by 'first principles' calculations. There is the added problem of attempting to focus the interest of physicists on 15 component systems! In the meantime, it seems clear that some parameterization in phenomenological descriptions will continue to be necessary although, hopefully, the magnitudes of the adjustable parameters required in such modeling will become smaller with the passage of time. Having said that, there is a clear need for the introduction of more physics into the methodology used in the current phenomenological calculations,[9] one which goes beyond the embrace of '*ab initio*' calculated zero-Kelvin total energies.

Several different contributions to the absolute entropies of alloy phases are possible. It is well known that, in pure metals, excitational entropy contributions often have a significant influence on the relative high-temperature stability of different allotropes. Entropy is much more important than enthalpy in determining excitational Gibbs energies, i.e., although the average excitational energy changes little as a function of temperature, the spread of available energy states increases substantially. Similar examples are found in the determination of the relative stability of different structures of stoichiometric compounds as a function of temperature; see Colinet et al.[10]

The excitational contributions to the entropy, S^{excit}, are also present in solution and non-stoichiometric compound phases but, in these cases, there are additional contributions to consider, viz., contributions from atom mixing (configurational), S^{config}, and from topological or positional effects, S^{posn}, due to local atomic relaxations and global volume changes which arise when the atoms are of disparate size. In the case of these phases, then, we may write the total entropy as

$$S = S^{\text{config}} + S^{\text{posn}} + S^{\text{excit}} \qquad \text{(Eq 1)}$$

The factorization given in Eq 1 is not to say that the different contributions can be regarded as independent. On the contrary, we might expect some coupling between them as when, for example, vibration excitations are influenced by local atom arrangements, i.e., S^{excit} may be influenced by S^{config}.

This article was presented at the Multi-Component Alloy Thermodynamics Symposium sponsored by The Alloy Phase Committee of the joint EMPMD/SMD of The Minerals, Metals, and Materials Society (TMS), held in San Antonio, Texas, March 12-16, 2006, to honor the 2006 William Hume-Rothery Award recipient, Professor W. Alan Oates of the University of Salford, UK. The symposium was organized by Y. Austin Chang of the University of Wisconsin, Madison, WI. Patrice Turchi of the Lawrence Livermore National Laboratory, Livermore, CA, and Rainer Schmid-Fetzer of the Technische Universitat Clausthal, Clauthal-Zellerfeld, Germany.

W. A. Oates, Institute for Materials Research, University of Salford, Salford M5 4WT, UK; Contact e-mail: aoates@globalnet.co.uk

In this article we will concentrate principally on S^{config} but, in order to emphasize the importance of the other contributions, we first make some brief observations about their importance.

2. Non-Configurational Entropy

For an ideal substitutional solution, the molar configurational entropy of mixing is given by

$$\Delta_{mix}S^{ideal} = -R\sum_i x_i \log_e(x_i) \quad \text{(Eq 2)}$$

The values obtained from this equation, which correspond with those for a random mixture, represent the upper limit for the configurational entropy of mixing. For binary systems, $\Delta_{mix} S^{config}$ lies in the range

$$0 \le \Delta_{mix}S^{config} \le +0.693\ R \quad \text{(Eq 3)}$$

where the upper limit is the value for a random equiatomic mixture. An excess entropy of mixing, S^E, is then defined as the difference between the property of a real solution and that for an ideal solution at the same composition:

$$S^E = \Delta_{mix}S - \Delta_{mix}S^{ideal} \quad \text{(Eq 4)}$$

The values of S^E for real alloys are often found to be quite significant. As an illustration, we show some results for fcc Au-Ni alloys in Fig. 1. These are taken from a recent assessment for this system at 1,200 K[11] and it can be seen that there is a substantial positive deviation from that for an ideal binary solid solution.

Another example, which shows both the integral formation and mixing quantities is given in Fig. 2. This figure shows integral entropy of formation, $\Delta_f S$, from two assessments for Al-Ni alloys at 1,500 K.[12,13] An ordered bcc phase is present around the equiatomic composition in these alloys and $\Delta_{mix}S$ for this phase can be obtained by relating the plotted values of $\Delta_f S$ for the bcc intermediate phase to the dotted curve which refers to the entropy of the phase-separated mixture of the pure metals with bcc structure. It can be seen that $\Delta_{mix}S$ for this phase is large and negative.

The results shown in Fig. 1 and 2 are not atypical. A survey from approximately 100 binary solid alloys[14] reveals that significant positive and negative values of $\Delta_{mix}S$, which are well outside the bounds given in Eq 3, are very often found in binary solid alloys.

It is clear from these examples that any thermodynamic modeling of solution phases which is based on configurational entropies alone is bound, in general, to be unsatisfactory for calculations involving real alloys. In the following, however, we will concentrate on the importance and modeling of the configurational contributions.

3. Configurational Entropy

3.1 Ideal Solutions

The simplest way of illustrating the effect of configurational entropy of mixing on high-temperature phase stability is summarized in the phase diagram shown in Fig. 3. The liquid phase is taken to be ideal, the solids to be immiscible, the melting points and entropies of fusion to be identical. It can be seen that the liquid phase region is most extensive at the mid-composition due to the fact that the configurational entropy is at its maximum there.

The upper limit of $\Delta_{mix}S^{config} = +0.693R$ for a binary system can be substantially exceeded in multicomponent alloys, as can be seen in the plot shown in Fig. 4, which results from using Eq 2 for different numbers of components. It can be seen that, in a ten-component system, the value of $\Delta_{mix}S^{config}$ can reach more than three times its value in a binary system.

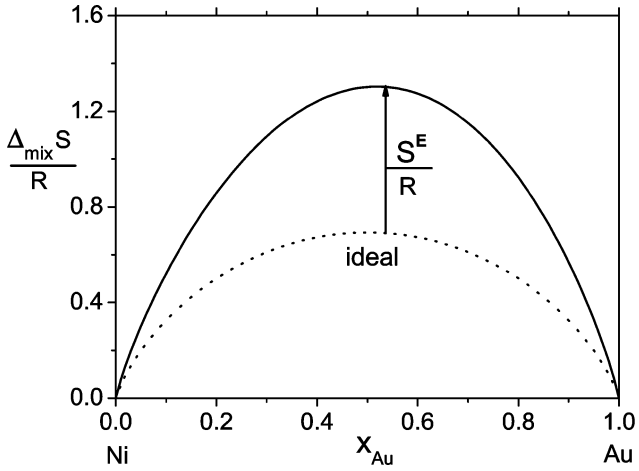

Fig. 1 Values for $\Delta_{mix}S$ for solid alloys for the fcc Au-Ni alloys at 1200 K taken from the assessment of Liu et al.[11]

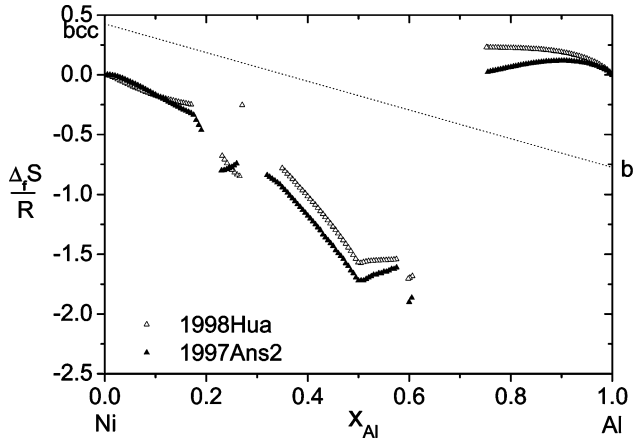

Fig. 2 Values for $\Delta_f S$ for solid alloys for the Al-Ni system at 1,500 K taken from two assessments.[12,13] The dotted line is for the phase separated mixture of bcc pure metals from which $\Delta_{mix}S$ can be obtained for the bcc phase present in alloys near the equiatomic composition

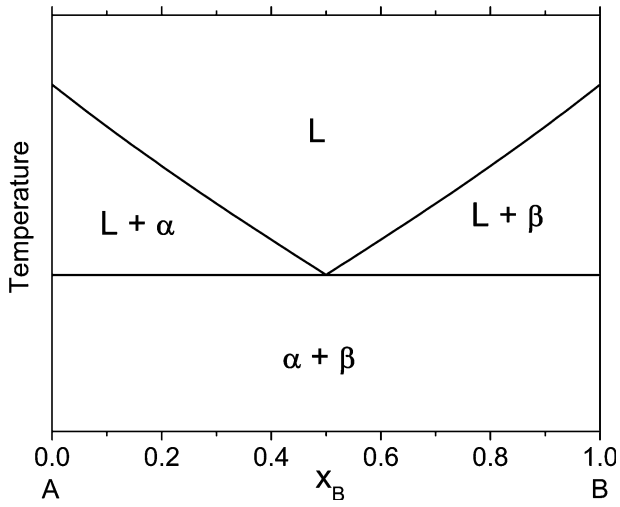

Fig. 3 Binary phase diagram for a simple eutectic system. The liquid phase is ideal; the pure solids, of identical melting points and entropies of fusion, are completely immiscible. The extent of the domain of phase stability of the liquid phase is determined by the magnitude of the configurational entropy of mixing

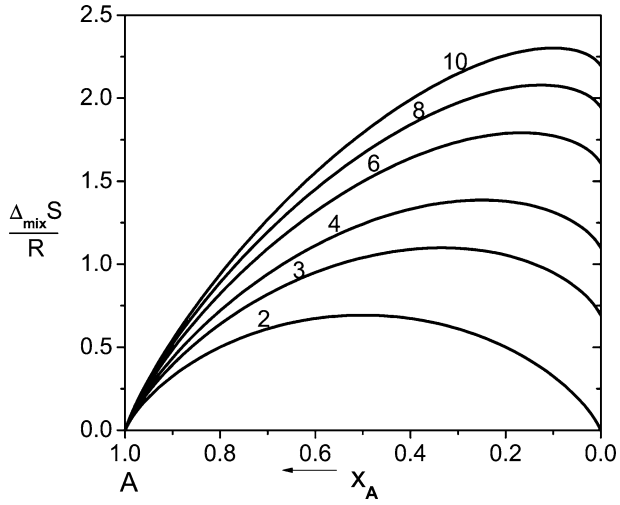

Fig. 4 Ideal configurational entropies of mixing for multicomponent alloys

Associated with the substantial increase in the maximum configurational entropy as the number of components increases, there is a concomitant depression in the eutectic temperature as can be seen in Fig. 5 and it is interesting to conjecture as to whether the increased phase stability brought about by configurational entropy stabilization in multicomponent solutions could be taken advantage of in, for example, the development of low temperature solders or bulk amorphous alloys. One group[15-17] have already appreciated this large effect in multicomponent alloys and have been looking at the possibility of exploiting it. They have made some interesting observations on the microstructures and mechanical properties of some AlCoCrCuFeNi alloys. The high values shown in Fig. 4 are unlikely to be too important in multicomponent alloys of general technological

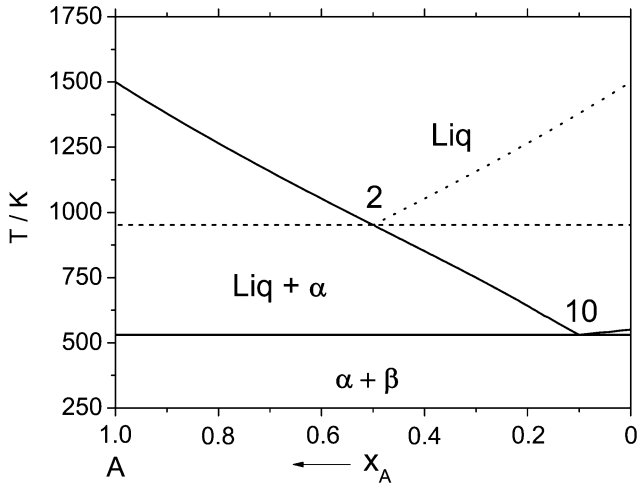

Fig. 5 Illustrating the increase, brought about by configurational mixing entropy, in the domain of stability of the liquid phase in a ten-component system as compared with a binary system. The liquid phase is assumed ideal; the solid phases are all immiscible

interest, since these are usually based on one component being present in a much higher concentration than the others.

The multicomponent effect may also manifest itself in a different, and perhaps undesirable, way. If a solution phase is metastable in a binary system and poorly described, then, due to the multicomponent configurational entropy effect, it may inadvertently and erroneously appear to be stable in the multicomponent system. Something along these lines may be occurring in the calculated presence of an fcc phase in the ternary Cu-Sn-Ni system at low Ni concentrations (U. Kattner, private communication, 2006). This phase is not stable in the binary Cu-Sn system and it is not clear as to whether a poor description there is responsible for it predicted presence in the ternary.

A less obvious illustration of the effect of S^{config} influencing the domain of stability of a solution phase is encountered in the case of the dissolution of an interstitial solute in a binary substitutional alloy. A specific example arises in the case of the terminal solubility of H (TSH) in solid solutions of Nb-Ta alloys. At a certain concentration of H in the solid solution phase a hydride phase becomes more stable. The experimental points shown in Fig. 6 show that there is a significant increase in the TSH in the alloys at 250 K as compared with the values in the pure metals.

In trying to understand results like those shown in Fig. 6, the role played by configurational entropy can be isolated by considering the simple example where it is assumed that the alloy host atoms, *A* and *B*, form an ideal substitutional solution and the H dissolves as an ideal interstitial solution in the substitutional alloy host.

In order to simplify the example further, we assume that there is only one interstitial site per metal atom. We also assume that, at the terminal solubility, the solid solution is in equilibrium with hydrides of composition AH(α) on the A-rich side and BH(β) on the B-rich side. Since AH(α) and BH(β) have different structures they are assumed to be completely immiscible.

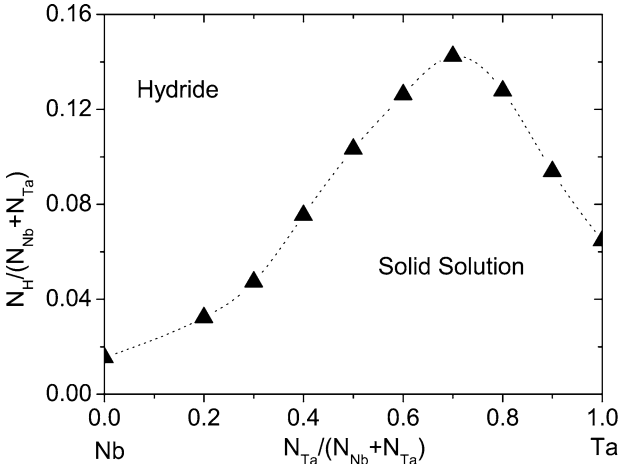

Fig. 6 Terminal solubility of H in contact with a hydride phase in Nb-Ta alloys at 250 K. The experimental results are taken from Ref 18.

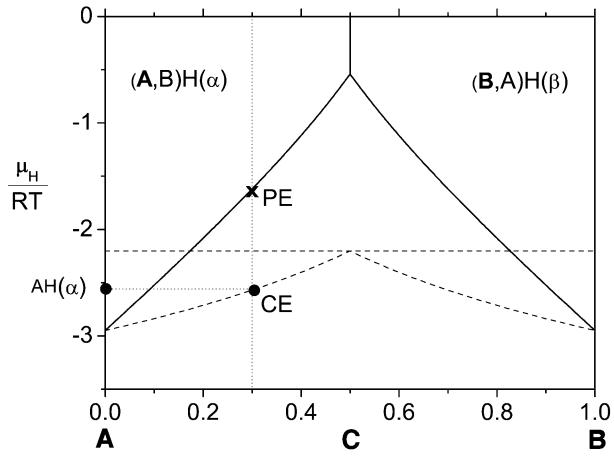

Fig. 7 Calculated variation of the hydrogen chemical potential at the TSH in a substitutionally ideal alloy host in which H dissolves as an ideal interstitial solution. The hydrides $AH(\alpha)$ and $BH(\beta)$ are assumed immiscible. The dashed curves refer to the complete equilibrium phase diagram, the solid curves to the para-equilibrium phase diagram

With these assumptions, the relative chemical potentials (the following quantities are in dimensionless units) for the three components are given by

$$\Delta_f\mu_H = \mu_H - \frac{1}{2}\mu^o_{H_2} = \Delta_f\mu^o_H + \log_e\left(\frac{r}{1-r}\right) \quad \text{(Eq 5)}$$

$$\mu_A - \mu^o_A = \log_e(1-c) + \log_e(1-r) \quad \text{(Eq 6)}$$

$$\mu_B - \mu^o_B = \log_e(c) + \log_e(1-r) \quad \text{(Eq 7)}$$

where $r = N_H/(N_A + N_B)$ and $c = N_B/(N_A + N_B)$.

For complete equilibrium (CE) between the solid solution phase and the hydride phase (indicated by the 'h' superscript) the chemical potentials for all three elements are equal in both phases:

$$\mu_H = \mu^h_H \quad ; \quad \mu_A = \mu^h_A \quad ; \quad \mu_B = \mu^h_B \quad \text{(Eq 8)}$$

The usual situation encountered, however, is one where the metal atoms are essentially frozen with only the H atoms mobile enough to be able to come to equilibrium between the two phases. In this case of para-equilibrium (PE), the alloy composition of the solid solution and hydride phases are identical and the last two equations must be replaced by

$$(1-c)\mu_A + c\mu_B = (1-c)\mu^h_A + c\mu^h_B \quad \text{(Eq 9)}$$

Solution of Eq 5-9 gives the following equations for CE and PE on the A-rich side:

$$\text{CE}: \quad \Delta_f\mu^o_H(A) + \log_e(r) + \log_e(1-c) = \Delta_f G^o(AH(\alpha)) \quad \text{(Eq 10)}$$

$$\text{PE}: \quad \Delta_f\mu^o_H(c) + \log_e(r) = \Delta_f G^o(MH(\alpha), c) \quad \text{(Eq 11)}$$

where

$$\Delta_f G^o(MH(\alpha), c) = (1-c)\Delta_f G^o(AH(\alpha)) + c\Delta_f G^o(BH(\alpha)) + \Delta_{mix}G \quad \text{(Eq 12)}$$

Here, the α-structural form of the hydride is the stable one on the *A*-rich side and *B* will be forced into this structural form when PE is present.

Results for this simple case of ideal solutions are shown in Fig. 7 and 8. The following (dimensionless) values for the quantities involved have been used in the calculation of Fig 6 and 8:

$$\Delta_f\mu^o_H(A) = \Delta_f\mu^o_H(B) = 0,$$

$$\Delta_f G^o(AH(\alpha)) = \Delta_f G^o(BH(\beta)) = -3, \quad \text{for the stable forms of the hydrides,}$$

$$\Delta_f G^o(AH(\beta)) = \Delta_f G^o(BH(\alpha)) = +1, \text{for the unstable forms.}$$

The tie-line between solid solution and hydride for the CE case at $c = 0.3$ is terminated by the two dots whilst that for the PE is terminated by the crosses. It can be seen that there is an enhanced solubility in the metastable PE situation.

Since we have considered the alloy to be ideal, for both the substitutional and the interstitial components (and the stable hydrides to be immiscible), the effects illustrated in these figures are due solely to the increased stability of the solid solution phase at intermediate alloy concentrations brought about by its configurational entropy of mixing. Topologically, the $\mu_H - c$ phase diagram is identical with the T–x phase diagram illustrated in Fig. 3 for a simple binary eutectic alloy.

The modeling of the results for a real system like H in Nb-Ta, as shown in Fig. 6, is more complicated than the simple case considered here, since, in the real system, both energy and non-ideal entropies come into play.

Because of the ability of the logarithmic nature of the configurational entropy term outweighing any finite energy contribution, it would also seem that there should always be an increase in *TSH* brought about by the addition of a

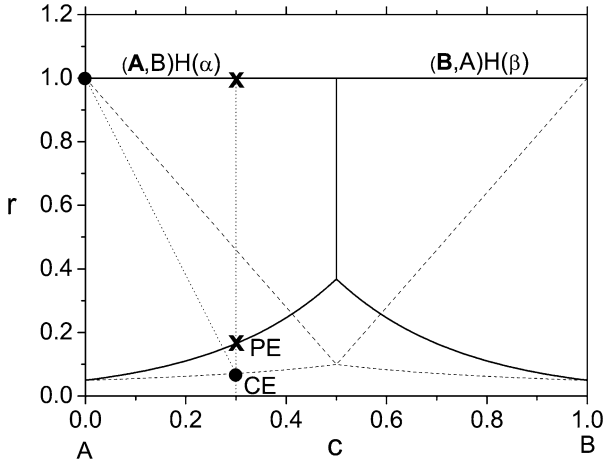

Fig. 8 Calculated variation of the TSH in a substitutionally ideal alloy host in which H dissolves as an ideal interstitial solution. The hydrides $AH(\alpha)$ and $BH(\beta)$ are assumed immiscible. The dashed curves refer to the complete equilibrium phase diagram, the solid curves to the para-equilibrium phase diagram

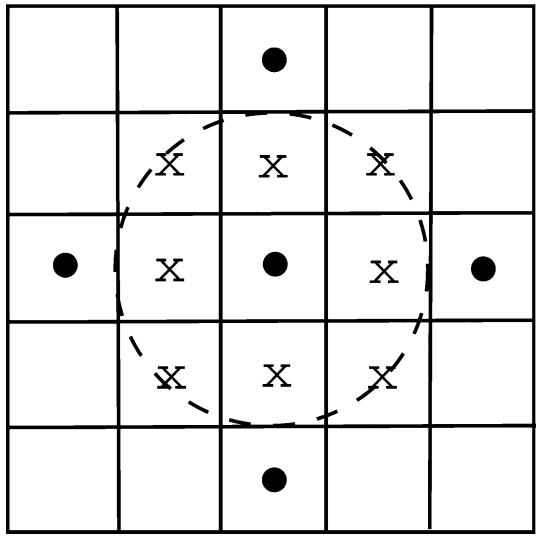

Fig. 9 'Halo' of blocked sites around an already occupied interstitial site due to large short-range H-H repulsive energies

substitutional solute to a host metal solvent. This appears to be in line with experimental observations, at least for Pd-based alloys.[19]

3.2 Athermal Solutions

Another instance of where the effects of configurational entropy can be completely isolated arises when the energy of mixing is zero, but the configurational entropy of mixing is not that for an ideal solution. Such solutions are described as being athermal.

We again consider an example involving a metal-hydrogen interstitial solid solution. The metal, M is taken to have the bcc structure with the H dissolving in the tetrahedral sites, of which there are six such interstitial sites per metal atom in the host lattice, $s = 6$.

If the solution is ideal, then the relative hydrogen chemical potential for the gas/solid equilibrium is given by:

$$\Delta_{\mathrm{f}}\mu_H = \mathrm{RT}\log_e\sqrt{p_{\mathrm{H_2}}} = \Delta_{\mathrm{f}}\mu_H^{\mathrm{o}}(T) + \mathrm{RT}\log_e\left(\frac{r}{s-r}\right) + \mu_H^{\mathrm{E}}(r,T) \qquad \text{(Eq 13)}$$

$\Delta_f\mu_H^{\mathrm{o}}$ is the non-configurational contribution at infinite dilution, the second term is from the ideal configurational entropy, and the composition-dependent excess quantity, μ_H^{E}, may contain both configurational and non-configurational contributions.

$\Delta_{\mathrm{f}}S_H$, $\Delta_{\mathrm{f}}S_H^{\mathrm{o}}$ and S_H^E can be obtained from the experimental results via the temperature derivatives of the relevant terms in Eq 13.

With $s = 6$, one might expect that the bcc phase would be stable over a wide composition range, but this is not found to be the case. Instead of being able to reach compositions approaching MH_6, as expected, it is found that the isotherms for p_{H2} versus r rise very steeply indeed at much lower H concentrations. It is now generally acknowledged that these experimentally observed low H saturation concentrations for H in bcc metals are due to large hard-core effects, i.e., there are large short-range H-H repulsive energies which may be of chemical and/or strain in origin. The effect, as shown schematically in Fig. 9, is to prevent future occupation of interstitial sites in close proximity to an already occupied interstitial site. Thus, each occupied interstitial site is surrounded by a 'halo' of blocked sites, and it is the influence of this 'blocking' on the configurational entropy which is principally responsible for the observed solubilities which are lower than those expected from using $s = 6$ for H in bcc metals like Zr, Ti, Nb, V and Ta.

In order to completely isolate the effect of configurational entropy, we consider the idealized case where it is assumed that there is an infinite repulsive energy between H atoms inside some defined radius together with a zero interaction energy outside this range. When the first H atom is inserted then there will be a complete halo of blocked sites surrounding it but, at higher H concentrations, the halos will overlap so that the average number of blocked plus occupied sites per inserted H atom, $\bar{z}$, will decrease with increasing H concentration. In the case of the blocking of the nearest and next nearest neighbor sites for H in tetrahedral sites in bcc metals, $\bar{z}$ varies from 7 at $r = 0$ to 4 at $r = 1.5$.

In order to simplify the model further, we assume that μ_H^E is zero, i.e., that any non-configurational contributions to μ_H are composition independent.

With these simplifying assumptions, the temperature derivative of Eq 13 is modified as follows:

$$\Delta_{\mathrm{f}}S_H == \Delta_{\mathrm{f}}S_H^{\mathrm{o}}(T) - R\log_e\left(\frac{r}{s-\bar{z}r}\right) \qquad \text{(Eq 14)}$$

The analytical calculation of $\bar{z}$ is difficult and is most conveniently carried out using Monte Carlo simulations.[20,21]

It is known from inelastic neutron scattering measurements of the optical mode frequencies for H in bcc metals that these correspond with Einstein temperatures in the region of 1,500 K. Actual experimental values can be used

in the calculation of S_H^o in the metal which, together with the gas phase properties, gives $\Delta_f S_H^o$. When Eq 14 (with $s = 6$ and blocking of nearest and next nearest neighbors) is used, the curve shown going through the points in Fig. 10 is obtained. If, on the other hand, it is assumed that $s = 1$ and that no blocking occurs, together with the same value of $\Delta_f S_H^o$, then the lower curve is obtained. As can be seen, the results calculated in this way are unsatisfactory with respect to both shape and position. It is necessary to use the proper crystallographic value of $s = 6$ and allow for blocking.

Some experimental results for $\Delta_f S_H$ in the case of H dissolved in Zr(bcc)[22] are shown in Fig. 10 as points. Whilst the simple model of the influence of blocking on configurational entropy gives a satisfactory explanation of the results shown in Fig. 10, real alloy situations can be more complex. Thus, whilst the nearest and next nearest neighbor sites seem to be always blocked, the magnitude of the repulsive energy between third nearest neighbors seems to be of the order *RT*, the effect of which is to cause a transition from third nearest neighbor site blocking at low temperatures to just second nearest neighbor site blocking at higher temperatures,[23] a transition which results in a Schottky-like heat capacity transition in V-H alloys.[21] This change in the size of the hard core with temperature presents extra difficulties for any physically realistic analytical blocking modeling for these phases.

4. Modeling Configurational Entropy in Multicomponent Solutions

All configurational solution models for solid alloys are based on Ising-like models and, for these, Monte Carlo (MC) simulations are very useful in that they can yield the 'exact' properties for a given set of energy parameters in those situations (most) where the exact result is not amenable to calculation. With the 'exact' results, it is then possible to assess the relative merits of different analytical models in their ability to reproduce the MC results using the same energy parameters. Comparison of the different calculated phase diagrams is a particularly useful way of ascertaining the quality of the entropy approximations, and this is the method of approximation assessment used here.

The most closely studied phase diagram by MC methods is that for the order/disorder transformations in fcc alloys when only constant nearest neighbor pair interactions are involved, and we will concentrate on this example here. The MC-calculated phase diagram for this system is shown as points in Fig. 11. The noticeable features in this diagram are the separated maxima for the $L1_0$ and $L1_2$ phases and a value for the triple-point temperature between $A1$, $L1_0$ and $L1_2$ phases of $-\mathrm{RT}/W_{AB} \approx 1$ (W_{AB} is the pair exchange energy defined by $W_{AB} = \varepsilon_{AB} - \frac{1}{2}(\varepsilon_{AA} + \varepsilon_{BB})$, where ε_{ij} is the nearest neighbor bond energy).

4.1 The Bragg-Williams Approximation

In the Calphad modeling of alloy sublattice phases, the Bragg-Williams (B-W) approximation is invariably used. In this approximation, it is assumed that the different atoms mix randomly on the sublattices where these exist or on the principal lattice when the phase is disordered. The attraction in using this approximation rests solely in its computational advantage, since the point probabilities are used in the minimization of the free energy functional.

The line diagram shown in Fig. 12 is obtained by using the B-W approximation for the case of nearest neighbor interactions on a four-sublattice fcc model.[24] It can be seen, however, that the phase diagram calculated in this way is vastly different from the 'exact' one. In the B-W diagram order/disorder transitions occur at too high a temperature, there is no separation of the $L1_0$ and $L1_2$ maxima occurs and no triple point is found. These differences are due entirely to the neglect of short-range order (SRO) in the B-W approximation. In order to correct for this limitation, extra empirical parameters are used to fit the phase boundaries in

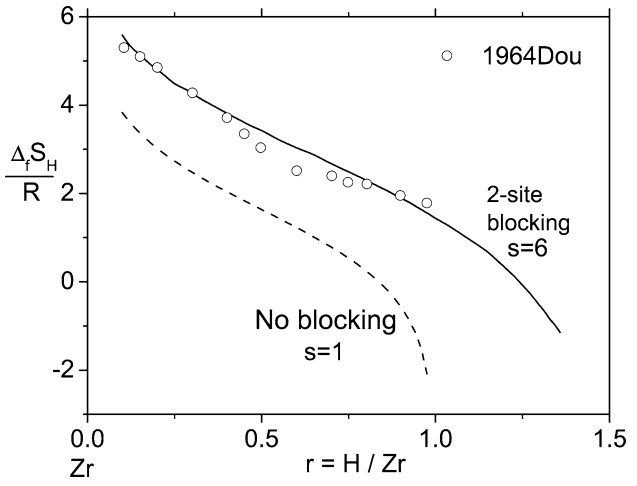

Fig. 10 Comparison of experimental and calculated values of ΔS_H for H in Zr(bcc) at 1,100 K. The solid curve was obtained by Monte Carlo simulations[20] and allows for site blocking of both nearest and next nearest neighbor T-sites; the dashed curve refers to no site blocking with $s = 1$ and with the same value of ΔS_H^o

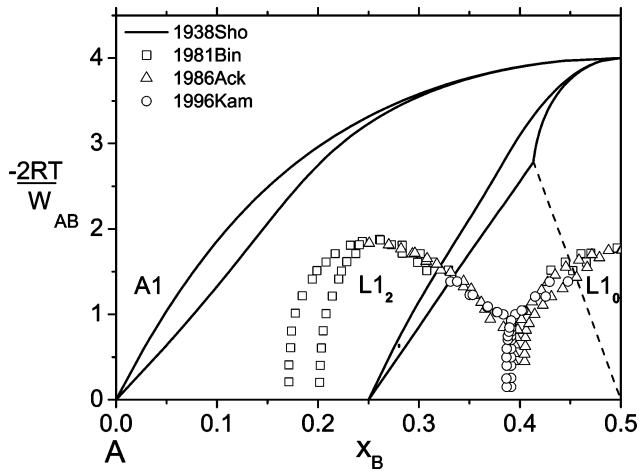

Fig. 11 Comparison of the 'exact' phase diagram with that calculated using a modified Compound Energy Formalism for fcc alloys with four sublattices

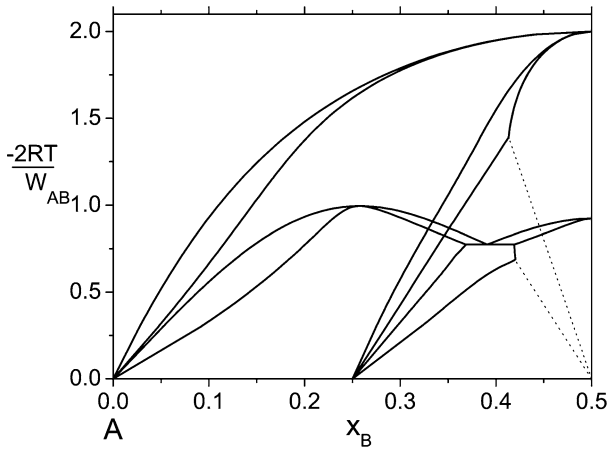

Fig. 12 Phase diagrams for fcc alloys with nearest neighbor pair interactions only. The line diagram is calculated using the B-W approximation; the points are the 'exact' phase diagram calculated using Monte Carlo methods

binary systems; the validity of using these same parameters for describing multicomponent systems seems questionable.

An alternative suggested approach is to use the modified Compound Energy Formalism (CEF).[25-30] This reproduces some of the *effects* of SRO, whilst not actually introducing it (it continues to use the B-W approximation). A phase diagram bearing a closer resemblance to the 'exact' one can be obtained through the medium of so-called reciprocal sublattice L parameters, which give additional contributions to the Gibbs energy. These parameters, of which there are 24 in total for a binary system, are permutations of terms like $y_A^{(1)}\, y_B^{(1)}\, y_A^{(2)}\, y_B^{(2)}\, y_A^{(3)}\, y_A^{(4)}\, L$, where $y_P^{(i)}$ is the sublattice mole fraction of component P on sublattice i. The effect including these parameters is to alter the enthalpy and, if the compound energies are temperature dependent, the non-configurational entropy of the disordered phase more strongly than they do for the ordered phase (for the fully ordered stoichiometric phase, the reciprocal sublattice L parameter contributions to G are zero). As can be seen in Fig. 11, this results in making the disordered phase relatively more stable, especially near the A_3 B and AB compositions, and hence lowers the disorder/order phase transition temperatures relative to those in the original B-W phase diagram. In doing so it also yields a phase diagram with separated maxima for the $L1_0$ and $L1_2$ phases, although one which is still some way off from having the topology of the 'exact' phase diagram at lower temperatures. It should also be noted that, because of the increased stability of the disordered phase, the enthalpy difference between ordered and disordered phases is reduced from that normally expected at an order/disorder transition. This problem is in addition to the weak assumption of no SRO in the disordered phase.

4.2 Higher-Order Approximations

In order to actually introduce SRO, it is necessary to use some better approximation than the B-W in the calculation of S^{config}. The most successful of the cluster methods has been the Cluster Variation Method (CVM),[31] but we will discuss others below. In all these cluster approximations, it is being assumed that the atomic interactions, within a range longer than the chosen basic cluster size, are negligible compared with the short-range interactions. This does not mean, though, that we need only consider a nearest neighbor pair cluster in the calculation of the configurational entropy when only nearest neighbor interactions are involved in the energy representation. In general, the larger the cluster selected for this purpose, the more accurate the calculated entropy. If, for the case of nearest neighbor interactions in the fcc lattice, a tetrahedron (T) cluster is selected in the calculation of the configurational entropy, then S^{config} is given by

$$\text{CVM, fcc, T-approxn.} \quad S^{\text{config}} = 2S_4 - 6S_2 + 5S_1 \qquad \text{(Eq 15)}$$

The cluster and sub-cluster configurational entropies in this and similar equations are given by

$$S_4 = -R \sum_{ijkl} p_{ijkl} \log_e p_{ijkl} \qquad \text{(Eq 16)}$$

p_{ijkl} being the cluster probability.

The second term in Eq 15 arises from the fact that, in the CVM, the tetrahedra share edges, and this leads to an overcounting of the total energy from the tetrahedra probabilities in the first term. The last term ensures that the total number of configurations is correct.

The use of the CVM T-approximation expression for S^{config} results in a free energy functional for a binary system which involves $2^4 - 1 = 15$ variables. Either the cluster probabilities or the correlation functions may be used in the free energy minimization. Herein lies the weakness of the CVM from the viewpoint of the materials engineer, viz., the large number of independent variables in the free energy functional when it is applied to multicomponent solutions. The number of equations to be solved can be in the order of C^n, where C is the number of components and n the number of atoms in the cluster.

A different expression for the configurational entropy results if it is assumed that the clusters are independent, i.e., share corners but do not share edges or faces. With this quasi-chemical approximation (QCA), a two-term expression for the configurational entropy is obtained:

$$\text{QCA, fcc, T-approxn.} \qquad S^{\text{config}} = S_4 - 3S_1 \qquad \text{(Eq 17)}$$

The number of functional variables, the cluster probabilities, in using this equation is the same as that in using Eq 15. A considerable reduction in this number is possible, however, by adapting the theory of gaseous atom/molecule equilibrium due to Fowler.[32] Yang and Li[33-36] used this approach (abbreviated to FYL below) to the site/cluster equilibrium in solids. Briefly, if the equilibrium constant and the atom/molecule mass balance are known, then the Helmholtz energy can be expressed in terms of the atom concentrations rather than the molecular concentrations. In using this method for transforming from the cluster probabilities to the site or point probabilities in a lattice comprising four sublattices, Lagrangian parameters are introduced as follows:

mass balances, $\log_e \lambda_1 \quad y_A^{(1)} = \sum_{jkl} p_{Ajkl}$

$\log_e \lambda_2 \quad y_A^{(2)} = \sum_{ikl} p_{iAkl}$

$\log_e \lambda_3 \quad y_A^{(3)} = \sum_{ijl} p_{ijAl}$

$\log_e \lambda_4 \quad y_A^{(4)} = \sum_{ijk} p_{ijkA}$

normalization, $\log_e \phi \quad \sum_{ijkl} p_{ijkl} = 1$

The introduction of the FYL transform into the QCA leads to the cluster/site approximation (CSA).[37,38] For a binary system, the number of functional variables is reduced, as is apparent from a comparison of the following equations for the configurational free energy:

$$\text{QCA} \quad F = \sum_{ijkl}^{16} p_{ijkl}(\varepsilon_{ijkl} + \log_e p_{ijkl}) - 3\sum_{P,i} \frac{1}{4} y_P^i \log_e y_P^i \qquad \text{(Eq 18)}$$

$$\text{CSA} \quad F = \sum_{i=1}^{4} y_A^i \log_e \lambda_i - \log_e \phi - 3\sum_{P,i} \frac{1}{4} y_P^i \log_e y_P^i \qquad \text{(Eq 19)}$$

The cluster partition function, ϕ, for a binary system, is related to the Lagrangian parameters through

$$\phi = \lambda_1\lambda_2\lambda_3\lambda_4 \exp(-\varepsilon_{AAAA}) + \ldots \quad \text{15 other terms} \qquad \text{(Eq 20)}$$

The equilibrium sublattice mole fractions are also directly related to the Lagrangian parameters:

$$y_A^i = \frac{1}{\phi}\frac{\partial \phi}{\partial \lambda_i} \qquad \text{(Eq 21)}$$

It can be seen from Eq 19 that FYL transform reduces the number of equations to only in the order of $C \times S$, where S is the number of sublattices. This is just the same as when using the B-W approximation.

Another cluster approximation should be mentioned. This is the constant coupling approximation (CCA), a pair cluster version of which was suggested originally by Kasteleijn and van Kranendonk.[39] It was later generalized and applied to T-clusters in bcc and fcc lattices by Bell.[40,41] In this approximation, edge and face sharing of the tetrahedra is permitted but, just as in the case of the QCA, a two-term entropy representation is used. In the case of the T-approximation for fcc lattices, Eq 15 is modified to

$$\text{CCA, fcc, T-approxn.} \quad S = 2S_4 - 7S_1 \qquad \text{(Eq 22)}$$

This equation may be used with cluster probabilities or, by carrying out the FYL transform, with point probabilities, i.e., equations analogous to either Eq 18 or Eq 19 may be used.

Results from using the CVM, QCA and CCA in the T-approximation are shown in Fig. 13 together with the MC results. The three approximations give rise to three different phase diagrams, with none of them being particularly close to the 'exact' one. It is clear why the QCA was discarded in favor of the CVM. Although the QCA introduces SRO and gives rise to the desired separation of the $L1_0$ and $L1_2$ maxima, it does not give a triple point between the $A1$, $L1_0$ and $L1_2$ phases in fcc alloys. It should also be noted that the triple point calculated in the T-approximation from the CCA is considerably poorer than that obtained from the CVM, although even that is disappointing. It is for this reason that larger clusters than the tetrahedron are recommended when using the CVM, although these are unsuitable for use with multicomponent systems.

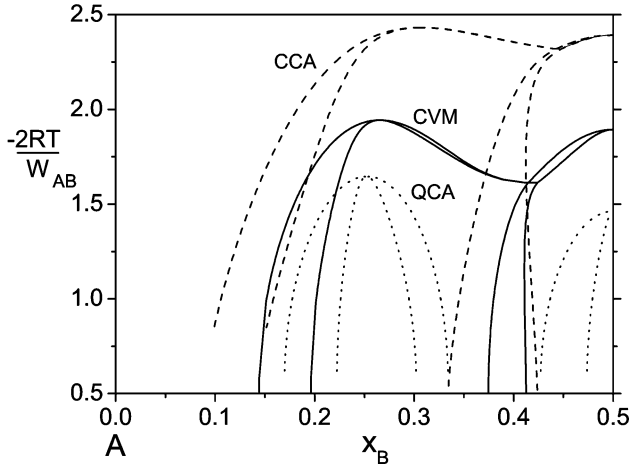

Fig. 13 Comparison of phase diagrams calculated using different configurational entropy approximations, all of which based on the nearest-neighbor tetrahedron cluster in the fcc lattice

In order to have the freedom of fitting to experimental (or calculated) results, a modified CSA has been proposed.[38] An adjustable parameter γ_4 with the dimensions of clusters per site is used so that Eq 14 is modified to read

$$\text{modified CSA} \quad S^{\text{config}} = \gamma_4 S_4 - (4\gamma_4 - 1)S_1 \qquad \text{(Eq 23)}$$

The γ_4 factor may be either obtained from MC simulations or, when dealing with real alloy systems in a phenomenological calculation, it can be regarded as a fitting parameter in the same way as are the energy parameters. With a value of $\gamma_4 = 1.23$ it is possible to obtain excellent agreement between the modified CSA-calculated phase diagram and the 'exact' one, as is shown in Fig. 14.

4.3 Further Use of the FYL Transform

Recently, we have extended the use of the modified CSA by considering the tetrahedron-pair cluster in fcc alloys.[42,43] Apart from its use of the empirical constant, γ, however, there is also the difficulty of finding corner-sharing cluster polyhedra which embrace every site and every bond in some lattices. It is much easier to find edge- and/or face-sharing polyhedra as used in the CVM.

In an effort to try and overcome the limitations of the modified CSA we have also been exploring the possibility of using the FYL transform more widely than used previously.[44,45] As an illustration, we mention its application to the case discussed above, viz., to the T-approximation in fcc lattices. The full expression for F in the CVM T-approximation for fcc lattices when using cluster probabilities is given by

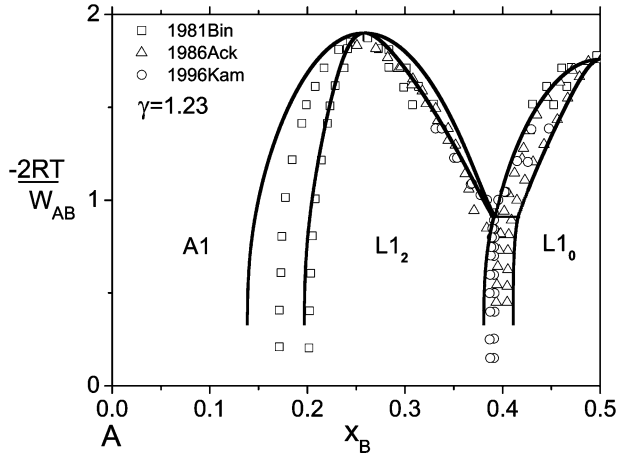

Fig. 14 Comparison of the modified CSA and 'exact' phase diagrams calculated using the T-approximation

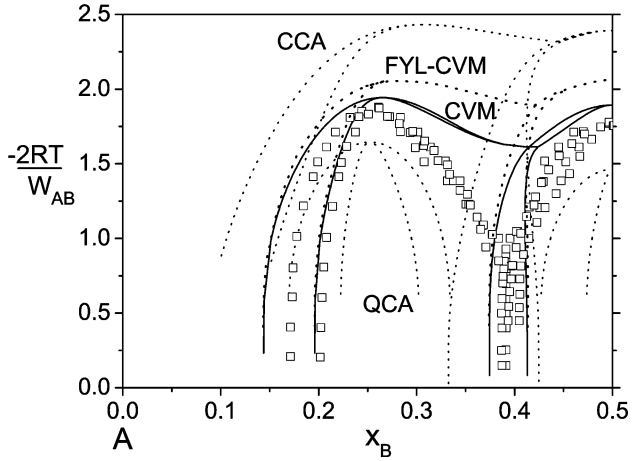

Fig. 15 Effect of using the Fowler-Yang-Li method on the calculated fcc phase diagrams in the T-approximation

$$\text{CVM} \quad F = 2\sum_{ijkl}^{16} p_{ijkl}(\varepsilon_{ijkl} + \log_e p_{ijkl}) - 6\sum_{ij}^{24}\frac{1}{6}p_{ij}(\varepsilon_{ij} + \log_e p_{ij}) + 5\sum_{P,i}\frac{1}{4}y_P^i \log_e y_P^i \qquad \text{(Eq 24)}$$

If an FYL transform is used in order to remove the tetrahedron probabilities, then the following expression for F is obtained:

$$\text{FYL}-\text{CVM} \quad F = 2\sum_{i=1}^{4}(y_A^i \log_e \lambda_i - \log_e \phi) - 6\sum_{ij}^{24}\frac{1}{6}p_{ij}(\varepsilon_{ij} + \log_e p_{ij}) + 5\sum_{P,i}\frac{1}{4}y_P^i \log_e y_P^i \qquad \text{(Eq 25)}$$

The tetrahedron probabilities can be obtained from the Lagrangian parameters, e.g., for p_{AAAA}:

$$p_{AAAA} = \frac{\lambda_1\lambda_2\lambda_3\lambda_4}{\phi}\exp(-\varepsilon_{AAAA}) \qquad \text{(Eq 26)}$$

The pair probabilities may then be obtained from the tetrahedron probabilities whilst the point probabilities can be obtained from Eq 21. These derived probabilities may then be inserted into Eq 25 and F minimized in terms of only four functional variables. The resulting phase diagram obtained from this procedure is shown in Fig. 15. It can be seen that, although the calculated phase diagram is not as good as that from a regular CVM calculation, it is considerably better than can be obtained from the CCA calculation.

Using the FYL transform in this way opens up the possibility of using much bigger clusters whilst still having only $C \times S$ functional variables. Its application to where correlation functions are used instead of cluster probabilities is also being explored.

5. Conclusions

- The phenomenological calculation of multicomponent phase diagrams is important for technological design. In order to be able to have the most confidence in the results from such calculations, it is important that the modeling equations used in the calculation of Gibbs energies for the various phases possess a sound physical basis so that they may be interpolated and extrapolated with some degree of confidence. On the other hand, the models used must be sufficiently simple that they are computationally economic. Extra adjustable parameters are an accepted necessity in these modeling equations. Their role is to allow for any unidentified or inadequately described factors and should, ideally, be both small and few in number.
- Entropies of mixing for binary solid alloys are frequently large, both positive and negative, indicating significant non-configurational contributions to the total entropy of a solution phase. These non-configurational entropies cannot be ignored in modeling.
- Configurational entropies can have a strong influence on the domain of stability of a solution phase.
- Allowing for short-range order in solution models is desirable in order to minimize the number of extra-fitting parameters required when the Bragg-Williams approximation is used. The great advantage of this approximation is its utilization of the point variables in the free energy functional mimimzation.
- Trying to modify the Bragg-Williams approximation in order to mimic the effect of short-range order, whilst not actually introducing it, is the least satisfactory way of doing this.
- The cluster variation method is the most widely recognized way of allowing for short-range order. Unfortunately, it utilizes too many functional variables, the cluster

probabilities, for it to be of value in the calculation of configurational entropies in multicomponent solutions.

- A Fowler-Yang-Li transform permits going from cluster probabilities to point probabilities, just as in the Bragg-Williams approximation. This results in the required large reduction in the number of functional variables. The modified cluster/site approximation, which utilizes this approach, is one way of using this transform to point variables.
- It seems possible that it will be possible to use the Fowler-Yang-Li transform more widely than hitherto.

References

1. W. Hume-Rothery, *The Metallic State: Electrical Properties and Theories*. Clarendon, Oxford, 1931
2. W. Hume-Rothery, *The Structure of Metals and Alloys*, Monograph and Report Series No 1, 1st ed., Institute of Metals, London, 1936
3. W. Hume-Rothery, *Atomic Theory for Students of Metallurgy*, Monograph and Report Series No 3, 1st ed., Institute of Metals, London, 1946
4. W. Hume-Rothery, *Electrons, Atoms, Metals and Alloys*. The Louis Cassier Co Ltd, London, 1948
5. W. Hume-Rothery, *The Structure of Alloys of Iron: An Elementary Introduction*. Pergamon, Oxford, 1966
6. W. Hume-Rothery, J.W. Christian, and W.B. Pearson, *Metallurgical Equilibrium Diagrams*. Institute of Physics, London, 1952
7. W. Hume-Rothery, R.E. Smallman, and C.W. Haworth, *The Structure of Metals and Alloys*, Monograph and Report Series No 1, 5th ed., Institute of Metals, London, 1969
8. W. Hume-Rothery and B.R. Coles, *Atomic Theory for Students of Metallurgy*, Monograph and Report Series No. 3, Institute of Metals, London, revised reprint of 3rd ed., 1969
9. W.A. Oates, H. Wenzl, and T. Mohri, On Putting More Physics into Calphad Solution Models, *CALPHAD*, 1996, **20**(1), p 37-45
10. C. Colinet, W. Wolf, R. Podloucky, and A. Pasturel, *Ab Initio* Study of the Structural Stability of $TiSi_2$ Compounds, *Appl. Phys. Lett.*, 2005, **87**, p 0419101-0419103
11. X.J. Liu, M. Kinaka, Y. Takaku, I. Ohnuma, R. Kainuma, and K. Ishida, Experimental Investigation and Thermodynamic Calculation of Phase Equilibria in the Sn-Au-Ni System, *J. Electronic Mat.*, 2005, **34**(5), p 670-679
12. I. Ansara, N. Dupin, H.L. Lukas, and B. Sundman, Thermodynamic Assessment of the Al-Ni System *J. Alloys Compd*., 1997, p 20-30
13. W. Huang and Y.A. Chang, A Thermodynamic Assessment of the Ni-Al System, *Intermetallics*, 1998, **6**, p 487-498
14. W.A. Oates and R. Schmid-Fetzer, 2007, to be published
15. J.-W. Yeh, S.-K. Chen, S.-J. Lin, J.-Y. Gan, T.-S. Chin, T.-T. Shun, C.-H. Tsau, and S.-Y. Chang, Nanostructured High-Entropy Alloys with Multiple Principal Elements: Novel Alloy Design Concepts and Outcomes, *Adv. Eng. Mater.*, 2004, **6**(4), p 299-303
16. C.-J. Tong, Y.-L. Chen, S.-K. Chen, J.-Y. Yeh, T.-T. Shun, C.-H. Tsau, S.-J. Lin, and S.-Y. Chang, Mechanical Performance of the AlCoCrCuFeNi High-Entropy Alloy System with Multi-Principal Elements, *Met. and Mat Trans. A.*, 2005, **36**(4), p 881-893
17. C.-J. Tong, M.-R. Chen, S.-K. Chen, J.-Y. Yeh, T.-T. Shun, S.-J. Lin, and S.-Y. Chang, Microstructure Characterization of AlCoCrCuFeNi High-Entropy Alloy System with Multi-Principal Elements, *Met. and Mat Trans. A*, 2005, **36**(5), p 1263-1271
18. D.G. Westlaked and J.R. Miller, Terminal Solubility of Hydrogen in Nb-Ta Alloys and Characterization of the Solid Solutions, *J. Less-Common Met*, 1979, **65**(1), p 139-154
19. Y. Sakamoto, F. Chen, M. Ura, and T. Flanagan, Thermodynamic Properties for the Solution of Hydrogen in Palladium-Based Binary Alloys, *Ber. Bunsenges fur Phys. Chem.*, 1995, **99**, p 807-820
20. W.A. Oates, J.A. Lambert, and P.T. Gallagher, Monte Carlo Computations of Configurational Entropies in Interstitial Solid Solutions, *Trans. Met. Soc AIME*, 1969, **245**, p 47-54
21. W.A. Oates, M. Hasebe, P. Meuffels, and H. Wenzl, Computer Experiments on the Thermodynamic Properties of the Primary Solid Solutions of Group vb Metal–Hydrogen Systems, *Z. fur Phys Chem. (N.F.)*, 1985, **146**, p 201-212
22. T.B. Douglas, Statistical Models for the Beta Zirconium Hydrides, *J. Chem. Phys.*, 1964, **40**, p 2248-2257
23. D.A. Faux and D.K. Ross, Tracer and Chemical Diffusion of Hydrogen in bcc Metals, *J. Phys. C: Solid State Phys.*, 1987, **20**, p 1441-1457
24. W. Shockley, Theory of Order for the Copper Gold Alloy System, *J. Chem. Phys.*, 1938, **6**(3), p 130-144
25. B. Sundman, S.G. Fries, and W.A. Oates, A Thermodynamic Assessment of the Au-Cu System, *CALPHAD*, 1998, **22**(3), p 335-354
26. A. Kusoffsky and B. Sundman, Thermodynamic Modeling of Short Range Order Using the Compound Energy Formalism, *Ber. Bunsenges. fiir Phys. Chem.*, 1998, **102**(9), p 1111-1115
27. A. Kusoffsky and B. Sundman, A Simplified Short Range Order Model Suitable for Multicomponent Alloys, *Z. Metallkd.*, 1998, **89**, p 836-839
28. A. Kusoffsky, Thermodynamic Evaluation of the Ternary Ag-Au-Cu System - Including a Short Range Order Description, *Acta Mater.*, 2002, **50**, p 5139-5145
29. A. Kusoffsky, N. Dupin, and B. Sundman, On the Compound Energy Formalism Applied to fcc Ordering, *CALPHAD*, 2002, **25**(4), p 549-565
30. T. Abe and B. Sundman, A Description of the Effect of Short Range Ordering in the Compound Energy Formalism, *CALPHAD*, 2003, **27**(4), p 403-408
31. R. Kikuchi, A Theory of Cooperative Phenomena, *Phys. Rev.*, 1951, **81**, p 988-1003
32. R.H. Fowler, *Statistical Mechanics*. Cambridge University Press, Cambridge U.K., 1938 162-164
33. C.N. Yang, A Generalisation of the Quasi-Chemical Method in the Statistical Theory of Superlattices, *J. Chem. Phys.*, 1945, **13**(2), p 66-76
34. C.N. Yang and Y. Li, General Theory of the Quasi-Chemical Method in the Statistical Theory of Superlattices, *Chinese J. Phys.*, 1947, **7**, p 59-71
35. Y. Li, Quasi-Chemical Theory of Order for the Copper–Gold Alloy System, *J. Chem. Phys.*, 1949, **17**(5), p 447-454
36. Y. Li, Quasi-Chemical Method in the Statistical Theory of Regular Mixtures, *Phys. Rev.*, 1949, **76**, p 972-979
37. W.A. Oates and H. Wenzl, The Cluster/Site Approximation for Multicomponent Solutions – A Practical Alternative to the Cluster Variation Method, *Scripta Mat.*, 1996, **35**(5), p 623-627
38. W.A. Oates, F. Zhang, S. Chen, and Y.A. Chang, An Improved Cluster/Site Approximation for the Entropy of Mixing in Multicomponent Solid Solutions, *Phys. Rev. B*, 1999, **59**, p 11221-11225

39. P.W. Kasteleijn, Constant Coupling Approximation for Ising Spin Systems, *Physica*, 1956, **22**, p 387-396
40. J.M. Bell and J. Oitmaa, Ordering in Binary fcc Alloys, *Physica A*, 1984, **129**, p 17-39
41. J.M. Bell, Modified Form of the Cluster Variation Method, *Phys. Rev. B*, 1987, **35**(8), p 3783-3789
42. W. Cao, J. Zhu, Y. Yang, R. Zhang, S.-L. Chen, W.A. Oates, and Y.A. Chang, Application of the Cluster/Site Approximation to fcc Phases in the Ni-Al-Cr System, *Acta Mater.*, 2005, **53**, p 4189-4197
43. Cao W., J. Zhu, R. Zhang, W.A. Oates, M. Asta, and Y.A. Chang, Application of the Cluster/Site Approximation to the Calculation of Coherent Interphase Boundary Energies, *Acta Mater.*, 2006, **54**, p 377-383
44. W.A. Oates, C. Colinet, 2007, to be published
45. C. Colinet and W.A. Oates, 2007, to be published